Creep tests on partially dried notched beams of silver fir wood (Abies alba)

Bontemps Arthur, G Godi, Rostand Moutou Pitti, Eric Fournely, Joseph J. Gril

World Conference on Timber Engineering Oslo 2023

CREEP TESTS ON PARTIALLY DRIED NOTCHED BEAMS OF SILVER FIR WOOD (ABIES ALBA)

Arthur Bontemps[1], Gaël Godi[2], Rostand Moutou Pitti[3,4], Eric Fournely[5], Joseph Gril[6,7]

ABSTRACT: Silver fir is an important species in the wood French industry but its application is facing drying issues. This paper presents the results of displacement-imposed bending tests and bending creep tests made on green or partially dried silver fir notched beams. The material consists in a batch of thirty beams that were characterised by measurements of basic density and longitudinal modulus of elasticity. The results suggest that the instantaneous strength is independent from the moisture content. During the creep tests, central deflection, crack parameters, shrinkage-swelling and meteorological parameters were measured. The time-dependent compliance is computed and takes into account crack propagation and multi-steps loading. The results show that the initial moisture content has an impact on the maximum time-dependent compliance reached but solar exposure and knots position are also significant parameters. The contribution of cracks to the deflection was also estimated and never exceeded 10% of the total deflection. Finally, observations showed that all crack trajectories were rising whatever the grain angle.

KEYWORDS: Creep, wood, Silver fir, notched beam, bending

1 INTRODUCTION

Silver fir (*Abies alba*) is an important species for European wood industry and accounts for 8% of the French forest. Its wood is mainly used in timber construction but is currently facing drying issues due to wetwood in Auvergne-Rhône-Alpes region [1]. Understanding and forecasting the mechanical behaviour of green or partially dried wood could promote the industrial development of new construction techniques. Traditional frameworks, made with undried wood for many centuries, could inspire the design of agricultural buildings or historical restoration. However, constraints imposed on building construction must be considered. Indeed, Eurocode 5 penalizes green wood by considering a higher final deflection, to account for mechano-sorptive effect resulting from drying under load [2]. However, creep of green timber structural elements depends on several complex factors that are not completely understood. There are several studies on green wood long-term mechanical properties, but mainly realised on small clearwood samples under controlled environments [3], [4]. This paper presents results of an experimental campaign on green or partially dried full-scale notched wooden beams in outdoor semi-sheltered conditions. Scientific challenges involve full-scale outdoor measurements and coupling between fracture mechanics and creep.

2 MATERIAL AND METHODS

2.1 NON-DESTRUCTIVE EXAMINATIONS

The material consists in a batch of 30 notched beams from local silver fir at structural element scale, Figure 1. Most of it is quarter sawn lumber (21/30), and the rest is rift sawn. The batch has been received in green wood state and characterised by non-destructive examination.

[1] Arthur Bontemps, Université Clermont Auvergne, CNRS, Clermont Auvergne INP, Institut Pascal, F-63000 Clermont-Ferrand, France, arthur.bontemps@uca.fr
[2] Gaël Godi, Université Clermont Auvergne, CNRS, Clermont Auvergne INP, Institut Pascal, F-63000 Clermont-Ferrand, France, gael.godi@uca.fr
[3] Rostand Moutou Pitti, Université Clermont Auvergne, CNRS, Clermont Auvergne INP, Institut Pascal, F-63000 Clermont-Ferrand, France, rostand.moutou_pitti@uca.fr
[4] Rostand Moutou Pitti, CENAREST, IRT, BP 14070, Libreville, Gabon
[5] Eric Fournely, Université Clermont Auvergne, CNRS, Clermont Auvergne INP, Institut Pascal, F-63000 Clermont-Ferrand, France
[6] Joseph Gril, Université Clermont Auvergne, CNRS, Institut Pascal, F-63000 Clermont-Ferrand, France, joseph.gril@cnrs.fr
[7] Joseph Gril, Université Clermont Auvergne, INRAE, PIAF, Clermont-Ferrand, France

https://doi.org/10.52202/069179-0074

Figure 1: *Beam dimensions (mm).*

2.1.1 Natural vibration tests

The BING© method has been used to measure longitudinal modulus of elasticity (MOE) and shear modulus. It consists in measuring the frequency spectrum of free vibrations of a beam and calculating the stiffness properties using the resonant frequencies. This test was realised before notching the beams. The dynamic MOE measured with this method is known to be 4% higher than the static one [5]. Results are given in Table 1. E^d is the dynamic MOE and G^d is the dynamic shear modulus in the longitudinal-tangential plane. It is observed that the batch is highly heterogeneous, E^d varying from 7.54 to 16.34 GPa.

Table 1: *Free vibration results*

	E^d [GPa]	G^d [GPa]
Minimum	7.54	0.451
Maximum	16.34	0.672
Mean	11.01	0.553
Standard deviation	2.3	0.055

2.1.2 Basic-density measurements

A thin slice of each beam where the green volume V_g and the ovendried mass m_{anh} were measured allowed to calculate the basic density as $\rho_{BD} = (m_{anh}/V_g)$.

The basic density is supposed to be an intensive property, hence the same for the thin slice and for the rest of the beam. As the beams were received in green wood state, their initial volume was V_g and the basic density allows to compute m_{anh} of the whole beams and thus the moisture content (MC) at each weighing. Finally, the basic specific modulus is computed as $E_S^d = (E^d/\rho_{BD})$. The results are given in Table 2.

Table 2: *Basic-density measurements, MC at receipt and* $\boldsymbol{E_S^d}$ *computations.*

	MC [%]	ρ_{BD} [kg.m^{-3}]	E_S^d [Mm^2.s^{-2}]
Minimum	25.1	333	21.49
Maximum	117.5	430	40.84
Mean	60.3	379	28.9
Std	23.9	27.4	4.7

The unit of E_S^d is Mm^2.s^{-2} as it is the square of the sound speed in the material [6]. It is observed that the initial MC is also highly heterogeneous, from 25.1% to 117.5%. However, the hypothesis that the beams are all initially in green state was not verified for every beam and led to approximate results of MC and E_S^d.

2.1.3 Repartition

The experimental campaign was divided into 4-points bending tests with incremental imposed displacement to study the strength as a function of MC, and 4-points bending creep tests to study the long-term mechanical evolution. Both types of tests were realised on wood above fibre saturation point (FSP, MC > 30%), partially dried wood (20% < MC < 30%) and dried wood (MC < 20%). For the creep tests 6 beams were loaded in Spring-Summer 2021, 6 in Autumn-winter 2021-2022 and 6 in Spring-Summer 2022. Figure 2 shows their repartition regarding their mechanical properties (E_S^d and ρ_{BD}). The whole range of mechanical properties has been tested at different MC.

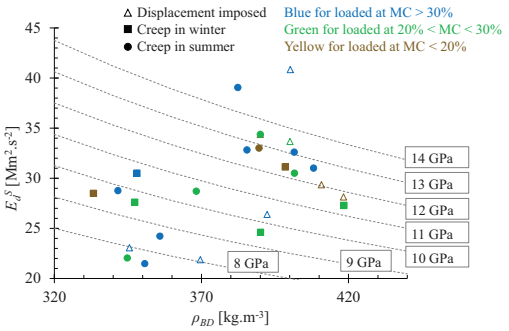

Figure 2: *Beam repartition plotted with specific modulus (*$\boldsymbol{E_S^d}$*) as a function of basic density (*$\boldsymbol{\rho_{BD}}$*). Filled circle: creep test in Summer; filled square: creep test in Winter; empty triangle: displacement-imposed test. Colours indicate initial moisture content (MC). Iso-module curves are added in grey dashed lines.*

2.2 BENDING TESTS

2.2.1 Displacement-imposed

The displacement-imposed 4-points bending tests were performed to correlate the strength with the initial MC and mechanical characteristics. The experimental set-up complies with the norm NF EN 408+A1 [7] and is represented in Figure 3. The central and intermediate deflections (respectively U_c, U_l and U_r) and the crack opening on the "left" and on the "right" (respectively C_{Ol} and C_{Or}) are measured using linear displacement transducers (LDT). The applied load is measured using two load cells.

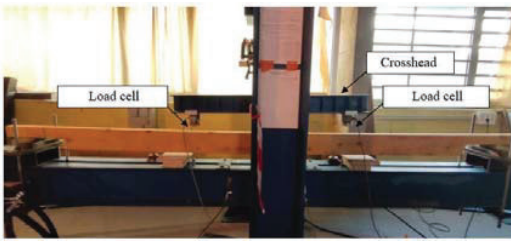

(a)

https://doi.org/10.52202/069179-0074

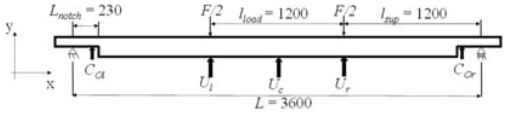

(b)

Figure 3: *Experimental set-up of the displacement-imposed tests: (a) picture of a test; (b) position of the devices. Numerical values are in millimetres.*

2.2.2 Creep tests

The creep tests aimed at studying the long-term mechanical behaviour of partially dried wood. The experimental set-up, shown in Figure 4, was in outdoor semi-sheltered conditions (i.e., sheltered from the rain but some beams were not sheltered from solar radiation). The load was applied using 350 kg waterproofed concrete blocks, incremented by 30 kg every month for 5 months and then every day, so that the duration of the tests never exceeded 7 months. Linear variable differential transformer (LVDT) sensors were used to measure the central deflection. A weather station close to the tests recorded temperature (T), relative humidity (RH) and solar radiation. Furthermore, two thermometers were stuck in the centre of each beam. A marker-tracking technique developed for these tests was used [8]. The relative displacement between markers allowed to measure the variation of beam height due to shrinkage-swelling and the crack opening, length and tip height.

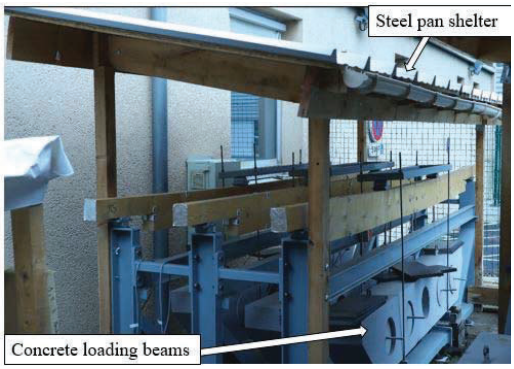

(a)

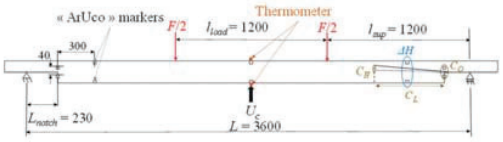

(b)

Figure 4: *Experimental set-up of creep tests: (a) picture of three loaded beams; (b) positions of measurement (values in mm).*

3 RESULTS AND DISCUSSION

3.1 INSTANTANEOUS RESPONSE

3.1.1 Comparison with non-destructive data

The displacement-imposed bending tests never exceeded 30 min and the mechanical response is hence considered as instantaneous. The axial stress is computed according to beam theory, and the strain, following [9], is given by:

$$\varepsilon \approx \frac{4\Delta U_{spa-r} H}{l_{load}^2} \quad (1)$$

where ε is the maximum normal strain in the centre of the beam, H the height of the beam, l_{load} the distance between the loading points and $\Delta U_{spa-r} = U_c - (U_l + U_r)/2$ the spatial-relative deflection. This allows to plot the stress-strain curves and calculate the static MOE with the slope of the linear part. An "instantaneous" central deflection of the creep tests was estimated by considering the central deflection at 10 minutes U_c^{10min}. An approach adapted from [10] allows computing the static MOE E using U_c^{10min} of the notched beam:

$$E = \frac{A \times f(\beta_0) \times \Delta F}{\Delta U_c^{10min}} \quad (2)$$

with:

$$A = \frac{23 l_{sup} L^2}{36 e H^3} \quad (3)$$

where e is the beam's thickness, L the beam length and l_{sup} the distance between support and loading point. Also:

$$f(\beta_0) = \left(1 + \frac{189\beta_0^3}{23}\right) \times \left[1 + \frac{108}{115}\left(\frac{H}{L}\right)^2 \left(\frac{E}{G}\right)^d \frac{1 + (3/2)\beta_0}{1 + (189/23)\beta_0^3}\right] \quad (4)$$

where $\beta_0 = (2L_{notch})/L$ is the notch factor. The comparison between the instantaneous results with the non-destructive examinations is given in Table 3.

Table 3: *Comparison between dynamic (E^d) and static (E) MOE. ΔE_{rel} corresponds to the relative difference such that $\Delta E_{rel} = (E^d\text{-}E)/E^d$.*

	E^d [GPa]	E [GPa]	ΔE_{rel} [%]
Minimum	7.54	6.02	-23
Maximum	16.34	13.96	32.8
Mean	11.25	9.74	12.4
Std	2.34	2.27	14.5

If the initial MC in a static test is below 30%, E is corrected by 0.15 GPa/% [11] as E^d is supposed to had been measured in green state. The relative difference $\Delta E_{rel} = (E^d\text{-}E)/E^d$ is explained by the natural dynamic and static difference and because E^d was measured on unnotched beams rather than E on notched beams.

3.1.2 Instantaneous strength

In Figure 5 the maximum force reached during the displacement-imposed tests is plotted as a function of ρ_{BD}, with the indication of MC.

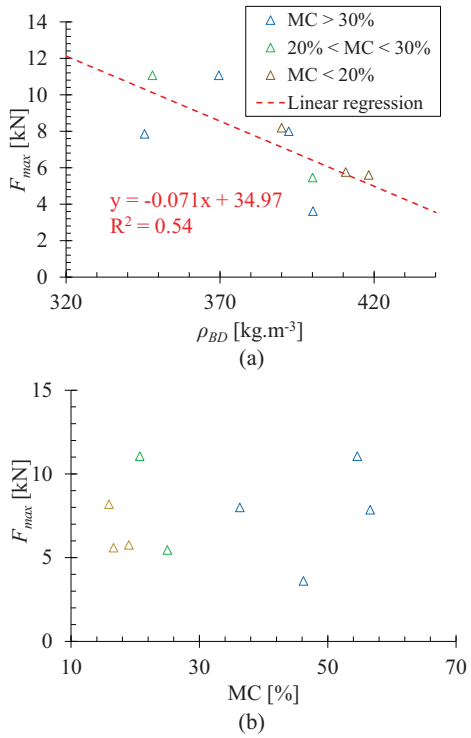

Figure 5: *Maximum force reached during the displacement-imposed tests: (a) as a function of the basic density; (b) as a function of MC.*

Although with a bad coefficient of determination ($R^2 = 0.54$, Figure 5(a)), F_{max} seems to be inversely proportional to ρ_{BD}. This is counterintuitive as the density should increase the MOE and thus F_{max}. As fracture mechanics occur in notched beams, it is supposed that a low MOE implicitly involves several knots that are reinforcements against crack propagation, increasing F_{max}. No correlation is observed between instantaneous F_{max} and initial MC of the tests, Figure 5(b).

3.2 DELAYED RESPONSE

3.2.1 Time-dependent deflection

The delayed response of the creep tests is observed using the time-relative central deflection $U_{time-r}(t)$ defined by:

$$U_{time-r}(t) = q(t) \times \frac{U_c(t) - U_c^{10min}}{U_c^{10min}} \qquad (5)$$

where $q(t)$ is the ratio of initial applied mass m_{ini} over total mass $m_{tot}(t)$ that is increased with load increments and the self-weight of the beam: $q(t) = m_{ini}/m_{tot}(t)$. The height variations due to shrinkage-swelling are measured by the marker tracking, hence correcting their impact on the central deflection: $U_c(t) = U_c(t) - \Delta H(t)/2$. Therefore, $U_{time-r}(t)$ is equivalent to the so-called K_{def} that takes creep into account in Eurocode 5, such that $U_{fin} = U_{inst}(1 + K_{def})$ for permanent load. For a class of service 3 (MC > 20% due to outdoor condition) and starting from green state, K_{def} is fixed at 3.

In Figure 6 the time-dependent deflection for all creep tests is plotted.

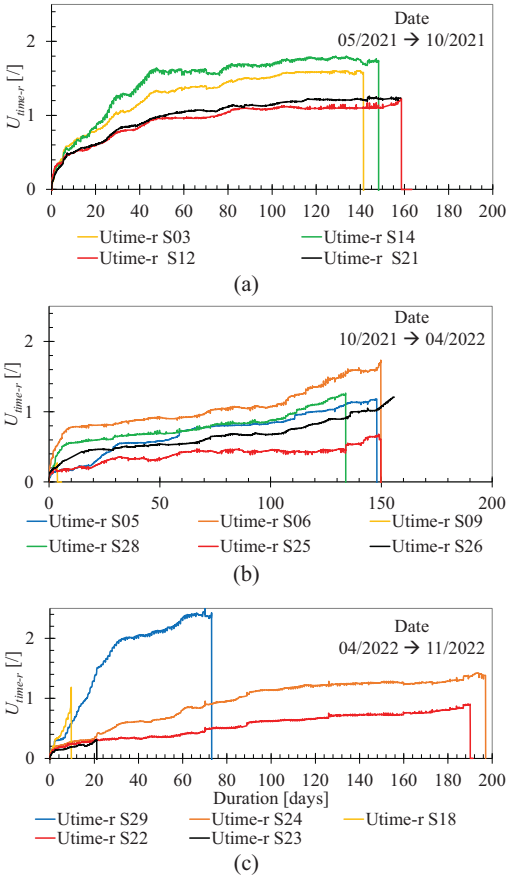

Figure 6: *Time-relative deflection as a function of time: (a) for the first 6 loaded beams in summer 2021; (b) for the 6 beams loaded in winter 2021-2022; (c) for the 6 beams loaded in summer 2022. Sij indicates the number of the considered beam.*

The measured time-dependent deflection never reached 3 as predicted for K_{def}, suggesting that it indeed integrates a safety factor. The beams loaded during Summer show on average a higher $U_{time-r}(t)$. Similar creep tests on initially dried silver fir wood never reached a time-dependent deflection above 2 for 2-years loading [9].

3.2.2 Time-dependent compliance

The time-dependent compliance J_{time-r} was calculated as:

$$J_{time-r} = \frac{E}{E(C_L, t)} - 1 \qquad (6)$$

where E is the initial computed MOE and $E(C_L, t)$ the stiffness evolution based on Equation (2), given by:

https://doi.org/10.52202/069179-0074

$$E(C_L, t) = \frac{A \times f(\beta) \times F(t)}{U_c(t)} \quad (7)$$

where *F(t)* is the updated applied force (adding load increments), $f(\beta)$ uses the crack factor β instead of β_0 by considering the crack length measurement as a notch extension:

$$\beta = \frac{2(L_{notch} + C_L)}{L} \quad (8)$$

This procedure discards the impact of crack propagation and load increments on J_{time-r} and allows comparing beams independently from these effects and from initial MOE. J_{time-r} should depends only on the wood creep itself that is impacted by MC and environmental conditions. In Figure 7 the maximum time-relative compliance reached is plotted as a function of the initial MC at the beginning of the creep test. The external beams exposed to solar radiation (Figure 4(a)) are indicated on the Figure as it has a significant impact on the maximum J_{time-r} reached.

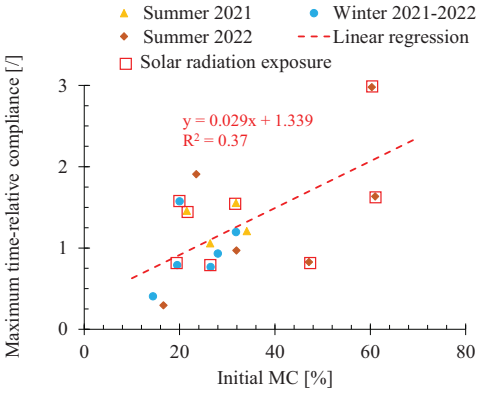

Figure 7: *Maximum time-relative compliance reached as a function of the initial MC at the beginning of the creep tests. Exposure to solar radiation is highlighted by red square.*

There is a slight tendency for the most dried beams to have a lower creep, but there is no strong correlation between initial MC at the beginning of a creep test and maximum time-relative compliance reached after 7 months ($R^2 = 0.37$). Exposure to solar radiations increases creep and brings an unpredicted factor in long-term wood mechanics. Therefore, it should be considered in the same way as moisture content.

3.3 FRACTURE MECHANICS

3.3.1 Deflection involved by fracture

Starting from the function of the notch factor β_0 in Equation (4), the ratio $f(\beta_0)/f(\beta)$, where β is the crack factor that supposes a crack propagation as a notch extension, can be defined. This ratio equals 1 if no crack occurred and decreases with crack propagation. Therefore, a "crack deflection" $U_{crack}(t)$, i.e., a deflection only due to crack propagation, is defined as:

$$U_{crack}(t) = U_c(t)\left(1 - \frac{f(\beta_0)}{f(\beta)}\right) \quad (9)$$

$U_{crack}(t)$ is the total deflection $U_c(t)$ minus the computed deflection as if the beam were free from crack. In Figure 8, $U_{crack}(t)$ is plotted as a function of time for two beams that represent the whole range of observed crack deflection. Thus, $U_{crack}(t)$ varies from 0.8 mm to 4.5 mm, that is at most about 10% of the total deflection. Although assumptions are strong in that computation, it is worth noting that crack seems to have a marginal impact on the observed deflection.

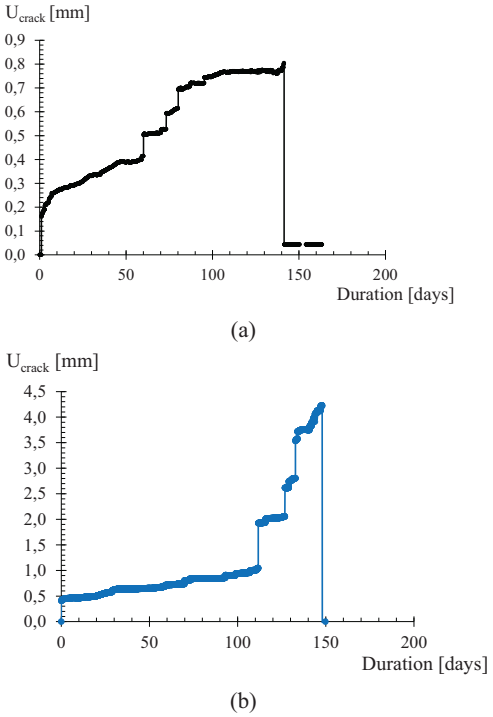

Figure 8: *Crack deflection as a function of time: (a) for beam S03 loaded in summer 2021 with few crack propagation; (b) for beam S05 loaded in winter with lots of crack propagation.*

3.3.2 Fracture facies observation

Observations of fracture facies were made a posteriori. In most cases beams with low strength but high stiffness were free from knots in the crack trajectory. On the contrary, high strength beams with low stiffness had either a knot into the trajectory or slanted facies, Figure 9(b)(c). Indeed, slanted facies requires more energy to propagates because surfaces that must be separated are larger. This result support the assumption that knots and anatomical configurations may increase a beam's strength. Furthermore, it is worth noting that all crack propagations occurred through rising toward the compression zone, whatever the grain angle (Figure 9(a)). It is surprising because the crack usually follows the grain. Reasons that may explain this observation are: (i) a descending crack would not break the beam but only

https://doi.org/10.52202/069179-0074

remove a piece; (ii) in a rising crack trajectory the section is progressively reduced and that is the opposite with a descending trajectory; (iii) in softwoods the overlapping of tracheids [12] allows a crack to rise slightly with no additional energetic cost.

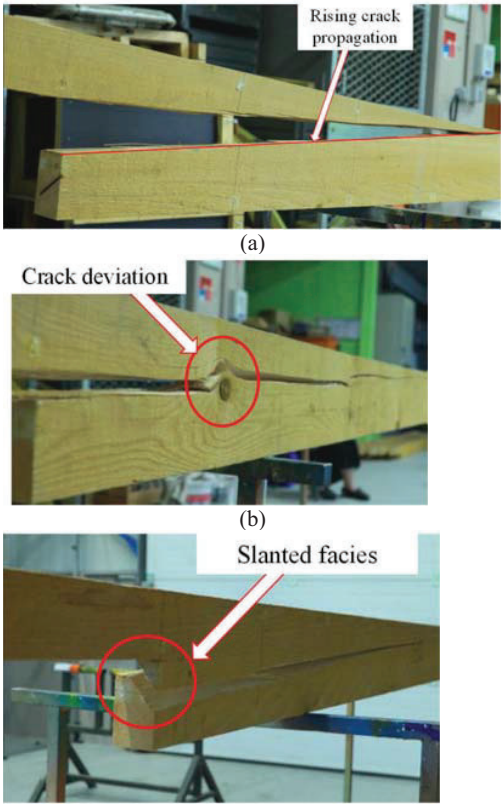

Figure 9: *Fracture facies observations: (a) A low strength beam with a rising crack propagation without knots; (b) crack deviation due to a knot; (c) a high strength beam with low basic density but slanted facies.*

4 CONCLUSION

This paper presents the results of an experimental campaign on full-scale notched beams of silver fir wood. Displacement-imposed bending tests and bending creep tests were realised on wood above FSP, partially dried and dried wood. The studied beam's batch is highly heterogeneous, but the experimental campaign is representative of the mechanical properties range. Both the dynamic and static MOE are consistent, but the estimated MC is not very accurate due to uncertainties on the green volume V_g. All other things being equal, initial MC has no visible impact on instantaneous strength. The basic density seems inversely proportional to that strength, and observations show that low basic density beams with high strength presented either knots on the crack trajectory or slanted facies that increased their strength. On the contrary, the time-dependent central deflection and compliance during creep tests tends to be proportional to the initial MC, but never exceed K_{def} proposed by Eurocode 5. This is explained by the important drying phase that increases the creep due to a mechano-sorptive effect. Nevertheless, exposure to solar radiation and knots position that resists to crack propagation also have a significant impact on the maximum time-relative compliance reached and have to be considered. The deflection only due to crack propagation was estimated to be less than 10% of the total deflection, meaning that crack has a marginal effect on the observed deflection. Finally, all fracture propagations rise whatever the grain angle. This is surprising and only intuitively explained: a rising crack propagation is energetically optimal. A finite element simulation of 4-points loaded notched beams may explain the rising crack trajectory.

ACKNOWLEDGEMENT

The authors would like to thank the Auvergne Rhône-Alpes region for the Ph.D. scholarship as well as the fundings of the Hub-Innovergne program of the Clermont Auvergne University.

REFERENCES

[1] L. Martin, H. Cochard, S. Mayr and E. Badel, "Using electrical resistivity tomography to detect wetwood and estimate moisture content in silver fir (Abies alba Mill.)," *Annals of Forest Science,* vol. 78, no. 65, 2021.

[2] D. Hunt, "A unified approach to creep of wood," *The Royal Society,* vol. 455, no. 1991, 1999.

[3] J. Dlouha, B. Clair, O. Arnould, P. Horacek and J. Gril, "On the time-temperature equivalency in green wood: Characterisation of viscoelastic properties in longitudinal direction," *Holzforschung,* vol. 63, no. 3, pp. 327-333, 2009.

[4] G. Pot, E. Toussaint, C. Coutand and J.-B. Le Cam, "Viscoelastic behaviour of maturing green poplar wood," in *SEM XIII International Congress and Exposition on Experimental and Applied Mechanics*, 2013.

[5] L. Brancheriau, Expertise mécanique des sciages par analyse des vibrations dans le domaine acoustique, Université Aix Marseille II, 2002.

[6] B. Thibaut and J. Gril , "Tree growth forces and wood properties," *Peer Community Journal Section: Forest & Wood Sciences,* 2021.

[7] AFNOR, "Structures en bois : Bois de structure et bois lamellé-collé. Détermination de certaines propriétés physiques et mécaniques," *NF EN 408+A1,* p. 38, 2012.

https://doi.org/10.52202/069179-0074

[8] A. Bontemps, G. Godi, E. Fournely , R. Moutou Pitti and J. Gril, “Implementation of an optical measurement method for monitoring mechanical behaviour. UNDER REVIEW,” *Experimental Techniques,* 2023.

[9] C. F. Pambou Nziengui, «Fissuration du bois en climat variable sous charges de longues durées : applications aux essences européennes et gabonaises,» Clermont-Ferrand, 2019.

[10] C. F. Pambou Nziengui, R. Moutou Pitti, E. Fournely , J. Gril, G. Godi and S. Ikogou, “Notched-beam creep of Douglas fir and white fir in outdoor conditions: Experimental study,” *Construction and Building Materials,* p. 13, 2019.

[11] D.Guitard, Mécanique du matériau bois et composites, 1987.

[12] M.-C. Trouy et P. Triboulot, «Matériau bois - Structure et caractéristiques,» *Techniques de l'ingénieur,* 2019.